A Hybrid Framework Combining Model-Based and Data-Driven Methods for Hierarchical Decentralized Robust Dynamic State Estimation

Marcos Netto, *Student Member, IEEE,* Venkat Krishnan, *Member, IEEE,* Lamine Mili, *Life Fellow, IEEE,* Yoshihiko Susuki, *Member, IEEE,* and Yingchen Zhang, *Senior Member, IEEE*

***Abstract*—This paper combines model-based and data-driven methods to develop a hierarchical, decentralized, robust dynamic state estimator (DSE). A two-level hierarchy is proposed, where the lower level consists of robust, model-based, decentralized DSEs. The state estimates sent from the lower level are received at the upper level, where they are filtered by a robust data-driven DSE after a principled sparse selection. This selection allows us to shrink the dimension of the problem at the upper level and hence significantly speed up the computational time. The proposed hybrid framework does not depend on the centralized infrastructure of the control centers; thus it can be completely embedded into the wide-area measurement systems. This feature will ultimately facilitate the placement of hierarchical decentralized control schemes at the phasor data concentrator locations. Also, the network model is not necessary; thus, a topology processor is not required. Finally, there is no assumption on the dynamics of the electric loads. The proposed framework is tested on the 2,000-bus synthetic Texas system, and shown to be capable of reconstructing the dynamic states of the generators with high accuracy, and of forecasting in the advent of missing data.**

***Index Terms*—Compressed sensing, data-driven dynamical systems, dynamic state estimation, Kalman filtering, Koopman mode decomposition, sparse selection.**

I. Introduction

The large-scale deployment of phasor measurement units (PMUs) and other grid-edge metering devices, such as smart meters [1] and micro-PMUs [2], is enabling the application of data analytics in electric power systems. This is fueling interest in data-driven methods that can enhance power system's reliability and resilience [3]. Simultaneously, and perhaps most importantly, we are witnessing an unprecedented increase in the share of renewable energy sources [4], [5], which are inherently intermittent and uncertain. The consequent increase in the stochastic dynamics of the net load challenges the traditional deterministic model-based, real-time monitoring and control methods applied in the legacy systems [6], [7]. Therefore, power engineers are looking to exploit the fast sampled measurement data to advance grid modeling, state estimation, forecasting, and controls through data analytics [8], [9], including by proposing data-driven dynamic state estimators (DSEs) [10], [11], which can track system dynamic states [12].

In this paper, we develop a two-level, hierarchical, decentralized, robust DSE by combining model-based and data-driven methods. The model-based decentralized DSEs at the lower level provide the necessary data for performing data-driven model identification at the upper level by using the Koopman mode decomposition (KMD) [13], which further allows for dynamic stability assessment and modal analysis of nonlinear dynamical systems [14]. The paper also illustrates the application of the proposed framework for large-scale systems by using compressed sensing [15] to find sparse state estimate selection. Because the use of all state estimates at the upper level could be prohibitive for high-dimensional systems, we rely on compressed sensing to find a sparse selection of state estimates, following the work of Brunton et al. [16], [17]. The proposed hybrid framework provides the opportunity to devise powerful tools by combining concepts from dynamical systems, estimation, and control theory. Firstly, the use of decentralized DSEs and KMD makes it independent of the network model; hence, it does not require a topology processor. Secondly, by virtue of the data-driven KMD, the method does not need to make assumptions about the underlying load model dynamics. Thirdly, and most notably, it can be completely embedded into the wide-area measurement systems instead of being an add-on to the energy management systems installed at the control centers. This attribute will ultimately facilitate the hierarchical control design of electric power systems [18] with the placement of control schemes at the phasor data concentrator (PDC) location, thereby exploiting the synergies between agile, low-latency, decentralized and holistic centralized monitoring and control architectures.

The paper proceeds as follows. Section II summarizes relevant literature and motivation for this work. Section III briefly introduces the data-driven robust DSE, and Section IV presents the sparse selection approach. Numerical results are discussed in Section V. The conclusions and directions for future research are given in Section VI.

II. Background and Motivation

Following the work of Modir and Schlueter [19], several DSEs [20]–[23] have been proposed based on the conceptual idea of transmitting all the PMU measurements to a centralized

This work was supported in part by CAPES Foundation, Ministry of Education of Brazil, under grant BEX13594/13-3.

This work was authored in part by the National Renewable Energy Laboratory (NREL), operated by Alliance for Sustainable Energy, LLC, for the U.S. Department of Energy (DOE) under Contract No. DE-AC36-08GO28308. Funding provided by the U.S. Department of Energy Office of Electricity (FIA181867). The views expressed in the article do not necessarily represent the views of the DOE or the U.S. Government. The U.S. Government retains and the publisher, by accepting the article for publication, acknowledges that the U.S. Government retains a nonexclusive, paid-up, irrevocable, worldwide license to publish or reproduce the published form of this work, or allow others to do so, for U.S. Government purposes.

M. Netto and L. Mili are with the Bradley Department of Electrical and Computer Engineering, Virginia Polytechnic Institute and State University, VA 22043 USA (e-mail: mnetto@vt.edu).

V. Krishnan and Y. Zhang are with the National Renewable Energy Laboratory (NREL), Golden, CO 80401 USA.

Y. Susuki is with the Department of Electrical and Information Systems, Osaka Prefecture University, Sakai, Osaka, Japan.

978-1-7281-1981-6/19/$31.00 ©2019 IEEE

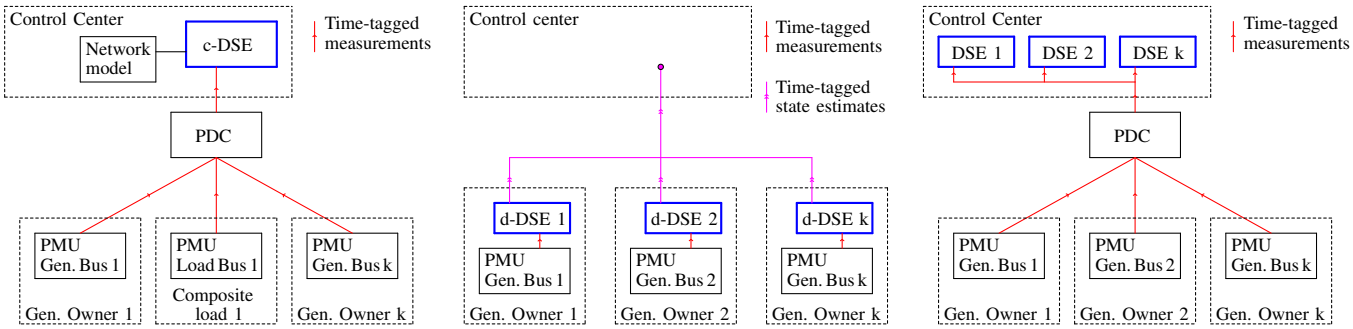

(a) Centralized DSE (c-DSE) (b) Decentralized DSE (d-DSE) (c) Centralized distributed DSE

Fig. 1. Comparison of the conceptual idea of different dynamic state estimators proposed in the literature. Note, in all the cases, system-level stability assessments such as inter-area oscillations [27], [28] will be done in a centralized manner, either supported by a centralized or decentralized DSE.

location, such as the control center, where the DSE is supposedly installed. We refer to this configuration as the centralized DSE; see Fig. 1a for more details. The assumptions are that the system is fully observable by PMUs and that the Kron-reduced network model (KNM) [24] is accessible. Although this may be true for independent system operators (ISOs) and regional transmission organizations (RTOs), access to the KNM is a hurdle for local utilities and transmission operators because of limited data sharing across neighboring systems. One alternative is to build dynamic reduced-order models [25]; unfortunately, this approach will increase the existing model uncertainties. Further, the KNM assumes that the electric loads are modeled as constant admittances, thereby not allowing for capturing the rich dynamics of composite electric loads [26]. Another important point that has been overlooked is that a topology processor is required to determine the KNM in real time; the existing topology processors embedded on the static state estimators cannot supply this demand. Nevertheless, although of reduced dimension, the graph of the KNM is full [24] rather than sparse, hence sparsity techniques cannot be exploited. The computational burden is another important barrier to the adoption of model-based centralized DSEs.

As an attempt to overcome the aforementioned problems, model-based decentralized DSEs have been investigated; see, for instance, [29], [30]. The idea is to individually estimate the states of each generator at their own location, as in Fig. 1b. Given that each decentralized DSE is designed for a particular generation location, only a PMU at the generator terminal is assumed. The decentralized DSE requires neither the model of the network nor the model of the electric loads, and it is computationally inexpensive because of a reduced number of involved state variables. Further, it offers the additional benefit of performing model calibration [31] without taking the generator offline, which is an appealing attribute from the system's reliability and economic standpoints. However, although a decentralized DSE allows for *local* stability assessment, control, and protection, for wide-area stability assessment and control, the DSE states will still need to be communicated to centralized processing, like any other architecture shown in Fig. 1; and, although the data transmissions in this case are not raw measurements but actual system states, it is still necessary to ensure data integrity, cybersecurity, and robustness against bad or missing information at the receiving end, i.e., at the control center. Additionally, in the event of loss of communication with a decentralized DSE, the states of the associated generator must be forecast. To circumvent some of these issues, Paul et al. [32] proposed a computationally distributed but physically centralized DSE, wherein the conceptual idea is to send all the measurements to a centralized location instead of performing the estimation separately for each generator; see Fig. 1c. Although ingenious, the approach in [32] relies on the reference signals of voltage and power that are accessible only to ISOs and RTOs, thereby precluding its adoption by transmission companies and alike utilities. The state forecasting capability is also not available.

Given the promise that decentralized DSEs have in terms of reducing the computational burden on increasing proliferations of sensors and data, and given its favorable trade-off between local and wide-area assessments, we delve deeper into the decentralized DSE. Presuming that model-based decentralized DSEs are available, we pose the following questions:

- Suppose that the state estimates are sent to a centralized location. How could one verify the data integrity of the received state estimates without relying on any model?
- How could one forecast the dynamic states in case of a communication problem with a given decentralized DSE?

To address these questions, we suggest the use of the robust, data-driven DSE, which is presented next.

III. Robust Koopman Kalman Filter

This section introduces the data-driven method, namely, the Koopman operator-based method that enables studying nonlinear dynamical systems without relying on any model. Further, the developed robust Koopman Kalman filter (KKF) [10], [11] lays the foundation for ensuring that the state estimates received from the decentralized DSEs will be robustly filtered.

A. The Koopman Operator

Consider a discrete-time autonomous dynamical system:

$$\boldsymbol{x}_k = \boldsymbol{f}(\boldsymbol{x}_{k-1}), \tag{1}$$

where the state $\boldsymbol{x}$ is an element of the state space $S \subset \mathbb{R}^n$, $\boldsymbol{f} : S \to S$ is the discrete map, and $k \in \mathbb{Z}$ is the time index. Define $\boldsymbol{g} : S \to \mathbb{R}$, a vector-valued observable in (1). The Koopman operator, $\mathcal{K}$, is a linear transformation on this vector space:

$$\mathcal{K}\boldsymbol{g}(\boldsymbol{x}_k) = \boldsymbol{g} \circ \boldsymbol{f}(\boldsymbol{x}_k) = \boldsymbol{g}(\boldsymbol{f}(\boldsymbol{x}_k)). \tag{2}$$

The Koopman eigenvalues, μ_i, and the Koopman eigenfunctions (KEFs), φ_i, of $\mathcal{K}$ are defined as follows:

$$\mathcal{K}\varphi_i(\boldsymbol{x}_k) = \mu_i \varphi_i(\boldsymbol{x}_k), \quad i = 1, 2, ... \tag{3}$$

If all the elements of $\boldsymbol{g}$ lie within the span of the KEFs, then we have:

$$\boldsymbol{g}(\boldsymbol{x}_k) = \sum_{i=1}^{\infty} \varphi_i(\boldsymbol{x}_k)\boldsymbol{\phi}_i = \sum_{i=1}^{\infty} \varphi_i(\boldsymbol{x}_0)\boldsymbol{\phi}_i \mu_i^k, \tag{4}$$

where $\boldsymbol{\phi}_i$ are the Koopman modes [13], and $\{\mu_i, \varphi_i, \boldsymbol{\phi}_i\}$, $i = 1, 2, ...$, are referred to as the Koopman tuples. The interested reader is referred to [13] for more details on the derivation of (4). For power systems, because of the existence of multiple attractors, we estimate a subset of the Koopman tuples, such that $\boldsymbol{g}(\boldsymbol{x}_k) \approx \sum_{i=1}^{q} \varphi_i(\boldsymbol{x}_k)\boldsymbol{\phi}_i = \sum_{i=1}^{q} \varphi_i(\boldsymbol{x}_0)\boldsymbol{\phi}_i \mu_i^k$.

B. Koopman Canonical Coordinates [33]

Consider the discrete-time autonomous dynamical system:

$$\boldsymbol{x}_k = \boldsymbol{f}(\boldsymbol{x}_{k-1}), \qquad \boldsymbol{y}_k = \boldsymbol{h}(\boldsymbol{x}_k), \tag{5}$$

where $\boldsymbol{x}$ and $\boldsymbol{f}$ are defined as in (1), $\boldsymbol{y} \in \mathbb{R}^m$ is the system observation vector, and $\boldsymbol{h} : S \to \mathbb{R}^m$. Let $\mathcal{F}^q = \text{span}\{\varphi_i\}_{i=1}^q$ be a subset of the KEFs, such that $\boldsymbol{x}, \boldsymbol{y} \in \mathcal{F}^q$. Then, we have:

$$\boldsymbol{x}_k \approx \sum_{i=1}^{q} \varphi_i(\boldsymbol{x}_{k-1})\boldsymbol{\phi}_i^{(\boldsymbol{x})}\mu_i, \quad \boldsymbol{y}_k \approx \sum_{i=1}^{q} \varphi_i(\boldsymbol{x}_{k-1})\boldsymbol{\phi}_i^{(\boldsymbol{y})}\mu_i. \tag{6}$$

Now, suppose that the Koopman tuples are ordered such that complex conjugate pairs appear adjacent to each other. It can be shown [11] that a nonlinear change of coordinates is given by $\mathcal{T}_{\mathcal{K}} : \mathbb{R}^n \to \mathbb{R}^q$, expressed as:

$$\mathcal{T}_{\mathcal{K}}(\boldsymbol{x}) = \underline{\boldsymbol{x}} = \left[\underline{x}_1, ..., \underline{x}_q\right]^\top, \tag{7}$$

where $\cdot^\top$ denotes the transpose of a vector,

$$\begin{cases} \underline{x}_i = \varphi_i, \text{ if } \varphi_i \text{ is real-valued,} \\ \underline{x}_i = 2\Re\{\varphi_i\} \text{ and } \underline{x}_{i+1} = -2\Im\{\varphi_i\}, \text{ if } (\varphi_i, \varphi_{i+1}) \\ \qquad \text{form a complex conjugate pair,} \end{cases}$$

$\Re\{\varphi_i\}$ and $\Im\{\varphi_i\}$ are the real and imaginary parts of φ_i, respectively. Using (7), and after some algebraic manipulation [11], we have:

$$\underline{\boldsymbol{x}}_k = \boldsymbol{\Omega}\, \underline{\boldsymbol{x}}_{k-1}, \quad \boldsymbol{x}_k = \boldsymbol{\Phi}^{(\boldsymbol{x})}\underline{\boldsymbol{x}}_k, \quad \boldsymbol{y}_k = \boldsymbol{\Phi}^{(\boldsymbol{y})}\underline{\boldsymbol{x}}_k, \tag{8}$$

and, remarkably, the nonlinear dynamical system in (5) can be mapped to the *linear* dynamical system (8). The KEFs define the Koopman canonical coordinates (KCC). If φ_i is real-valued, $\Omega_{i,i} = \mu_i$. If $(\varphi_i, \varphi_{i+1})$ form a complex conjugate pair, then we have:

$$\begin{bmatrix} \Omega_{i,i} & \Omega_{i,i+1} \\ \Omega_{i+1,i} & \Omega_{i+1,i+1} \end{bmatrix} = \begin{bmatrix} \Re\{\mu_i\} & \Im\{\mu_i\} \\ -\Im\{\mu_i\} & \Re\{\mu_i\} \end{bmatrix},$$

and, thus, $\boldsymbol{\Omega}$ is a block diagonal matrix.

The matrix $\boldsymbol{\Phi}^{(\boldsymbol{x})} \in \mathbb{R}^{n\times q}$ is a mapping between the states in the KCC, $\underline{\boldsymbol{x}}$, and the original state space coordinates, $\boldsymbol{x}$. If φ_i is real-valued, $\boldsymbol{\Phi}_{:,i}^{(\boldsymbol{x})} = \boldsymbol{\phi}_i^{(\boldsymbol{x})}$. Conversely, if $(\varphi_i, \varphi_{i+1})$ form a complex conjugate pair, $\boldsymbol{\Phi}_{:,i}^{(\boldsymbol{x})} = \Re\{\boldsymbol{\phi}_i^{(\boldsymbol{x})}\}$, $\boldsymbol{\Phi}_{:,i+1}^{(\boldsymbol{x})} = \Im\{\boldsymbol{\phi}_i^{(\boldsymbol{x})}\}$.

The matrix $\boldsymbol{\Phi}^{(\boldsymbol{y})} \in \mathbb{R}^{m\times q}$ is a mapping between the states in the KCC, $\underline{\boldsymbol{x}}$, and the observation vector in the original state space coordinates, $\boldsymbol{y}$. If φ_i is real-valued, $\boldsymbol{\Phi}_{:,i}^{(\boldsymbol{y})} = \boldsymbol{\phi}_i^{(\boldsymbol{y})}$. If $(\varphi_i, \varphi_{i+1})$ form a complex conjugate pair, $\boldsymbol{\Phi}_{:,i}^{(\boldsymbol{y})} = \Re\{\boldsymbol{\phi}_i^{(\boldsymbol{y})}\}$, $\boldsymbol{\Phi}_{:,i+1}^{(\boldsymbol{y})} = \Im\{\boldsymbol{\phi}_i^{(\boldsymbol{y})}\}$.

C. Robust Koopman Kalman Filter

In the KKF form, (8) becomes:

$$\begin{aligned} \underline{\boldsymbol{x}}_k &= \boldsymbol{\Omega}\underline{\boldsymbol{x}}_{k-1} + \boldsymbol{w}_{k-1}, \\ \boldsymbol{y}_k &= \boldsymbol{\Phi}^{(\boldsymbol{y})}\underline{\boldsymbol{x}}_k + \boldsymbol{v}_k, \end{aligned} \tag{9}$$

where $\boldsymbol{w}$ stands for the system process error, and $\boldsymbol{v}$ denotes the measurement noise. In what follows, we rely on [34] to solve (9). The interested reader is referred to [11] for details on the derivation of the robust KKF.

Now, the practical experience suggests that the synchronous generators oscillate coherently; see Fig. 2. This is equivalent of saying that the dynamics of electrical power systems evolve on a low-dimensional attractor. In the next section, this property is leveraged to perform a sparse selection of the state estimates used to identify the KKF, which is applicable to larger power systems.

IV. Sparse Selection of State Estimates

Following Manohar et al. [17], suppose that a state $\boldsymbol{x}$ evolving according to the nonlinear dynamics (1) has a compact representation in a transform basis $\boldsymbol{\Psi}$. In a universal basis $\boldsymbol{\Psi} \in \mathbb{R}^{n\times n}$, $\boldsymbol{x}$ might have a sparse representation:

$$\boldsymbol{x} = \boldsymbol{\Psi}\boldsymbol{s}, \tag{10}$$

$\boldsymbol{s} \in \mathbb{R}^n$ is a sparse vector. In a tailored basis $\boldsymbol{\Psi}_r \in \mathbb{R}^{n\times r}$, such as a basis defined by a proper orthogonal decomposition, $\boldsymbol{x}$ might have a low-rank representation:

$$\boldsymbol{x} = \boldsymbol{\Psi}_r\boldsymbol{\ell}, \tag{11}$$

$\boldsymbol{\ell} \in \mathbb{R}^r$. We seek to find a matrix $\boldsymbol{C} \in \mathbb{R}^{p\times n}$ consisting of a small number $(p \ll n)$ of optimized measurements:

$$\boldsymbol{b} = \boldsymbol{C}\boldsymbol{x}, \tag{12}$$

$\boldsymbol{b} \in \mathbb{R}^p$, which facilitates the accurate reconstruction of $\boldsymbol{s}$ or $\boldsymbol{\ell}$, and thus $\boldsymbol{x}$. Note that $\boldsymbol{C} = [\boldsymbol{e}_{\gamma_1}\, \boldsymbol{e}_{\gamma_2} ... \boldsymbol{e}_{\gamma_p}]^\top$, where $\boldsymbol{e}_{\gamma_i}$ is the unit vector with a unit entry at index γ_i and zeros elsewhere. Combining (10) and (12) yields:

$$\boldsymbol{b} = (\boldsymbol{C}\boldsymbol{\Psi})\,\boldsymbol{s} = \boldsymbol{\theta}\boldsymbol{s}. \tag{13}$$

Eq. (13) is referred to as the compressed sensing problem. Conversely, combining (11) and (12) yields:

$$\boldsymbol{b} = (\boldsymbol{C}\boldsymbol{\Psi}_r)\,\boldsymbol{\ell} = \boldsymbol{\theta}\boldsymbol{\ell}. \tag{14}$$

If $\boldsymbol{C}$ is properly structured such that $\boldsymbol{\theta}$ is well conditioned, it is possible to solve for the low-rank coefficients $\boldsymbol{\ell}$ given the measurements $\boldsymbol{b}$ in (14) as follows:

$$\hat{\boldsymbol{\ell}} = \begin{cases} \boldsymbol{\theta}^{-1}\boldsymbol{b} = \left(\boldsymbol{C}\boldsymbol{\Psi}_r\right)^{-1}\boldsymbol{b}, & p = r, \\ \boldsymbol{\theta}^{\dagger}\boldsymbol{b} = \left(\boldsymbol{C}\boldsymbol{\Psi}_r\right)^{\dagger}\boldsymbol{b}, & p > r, \end{cases} \tag{15}$$

$\boldsymbol{\theta}^\dagger$ denotes the Moore-Penrose pseudoinverse of $\boldsymbol{\theta}$. Thus, $\boldsymbol{x}$ can be estimated as $\hat{\boldsymbol{x}} = \boldsymbol{\Psi}_r\hat{\boldsymbol{\ell}}$. From (15), one seeks columns of $\boldsymbol{\Psi}_r$ corresponding to point sensor locations in the state space, $\boldsymbol{e}_{\gamma_i}$, that optimally condition the inversion of the matrix $\boldsymbol{\theta}$. The structure of the elements $\boldsymbol{e}_{\gamma_i}$ affect the condition number of $\boldsymbol{C}$ and consequently of $\boldsymbol{M}_{\boldsymbol{\gamma}} = \boldsymbol{\theta}^\top\boldsymbol{\theta}$. The condition number of the system might be indirectly bounded by optimizing the

spectral content of $\boldsymbol{M}_{\boldsymbol{\gamma}}$ using its determinant, trace, or spectral radius. For example, we have:

$$\begin{aligned}\boldsymbol{\gamma}_* &= \arg\max_{\boldsymbol{\gamma},|\boldsymbol{\gamma}|=p} |\det \boldsymbol{M}_{\boldsymbol{\gamma}}| = \arg\max_{\boldsymbol{\gamma}} \prod_i |\lambda_i(\boldsymbol{M}_{\boldsymbol{\gamma}})| \\ &= \arg\max_{\boldsymbol{\gamma}} \prod_i \sigma_i(\boldsymbol{M}_{\boldsymbol{\gamma}}), \end{aligned} \tag{16}$$

where λ_i and σ_i are, respectively, the i-th eigenvalue and singular value of $\boldsymbol{M}_{\boldsymbol{\gamma}}$. The QR factorization with column pivoting decomposes a matrix $\boldsymbol{M}_{\boldsymbol{\gamma}} \in \mathbb{R}^{m\times n}$ into a unitary matrix $\boldsymbol{Q}$, an upper triangular matrix $\boldsymbol{R}$, and a column permutation matrix $\boldsymbol{C}$, that is:

$$\boldsymbol{M}_{\boldsymbol{\gamma}}\boldsymbol{C}^\top = \boldsymbol{Q}\boldsymbol{R}. \tag{17}$$

The key idea from [17] is, when applied to an appropriate basis, the QR pivoting procedure provides an approximate greedy solution method for the optimization in (16), also known as a submatrix volume maximization because the matrix volume is the absolute value of the determinant.

A. Sparse Selection of State Estimates

In [17], the QR pivoting procedure is proposed as a tool to optimize sensor placement, in particular for the reconstruction of high-dimensional states from point measurements given tailored bases. Instead of measurements, here, we have access to the state estimates received from the robust, model-based, decentralized DSEs. Our objective is to shrink the number of state estimates used by the robust KKF so as to speed up its processing.

Algorithm 1 Sparse selection of state estimates

procedure
  $\boldsymbol{\Psi}_r \leftarrow \text{svd}(\hat{\boldsymbol{x}})$
  if $p == r$ **then**
    $\boldsymbol{\gamma} \leftarrow pivot(\boldsymbol{\Psi}_r)$ ▷ $[Q, R, pivot] = \text{qr}(\boldsymbol{\Psi}_r)$
  else if $p > r$ **then**
    $\boldsymbol{\gamma} \leftarrow pivot(\boldsymbol{\Psi}_r\boldsymbol{\Psi}_r^\top)$ ▷ $[Q, R, pivot] = \text{qr}(\boldsymbol{\Psi}_r\boldsymbol{\Psi}_r^\top)$
  $\boldsymbol{b} \leftarrow \hat{\boldsymbol{x}}_{\boldsymbol{\gamma}}$ ▷ $\hat{\boldsymbol{x}}_{\boldsymbol{\gamma}} = \hat{\boldsymbol{x}}_{\gamma_1:\gamma_p}$

After $\boldsymbol{b}$ is determined as in Algorithm 1, we make use of (7) such that:

$$\mathcal{T}_{\mathcal{K}}(\boldsymbol{b}) = \underline{\boldsymbol{x}} = \left[\underline{x}_1, ..., \underline{x}_q\right]^\top. \tag{18}$$

V. Numerical Results

We carry out simulations on the 2,000-bus synthetic Texas system [35] comprising 544 synchronous and 87 non-synchronous generators; the latter are modeled as variable-speed wind generators with full converters and do not contribute to the electromechanical modes. A three-phase short-circuit is applied to Bus 1017 and cleared after 10 milliseconds. Fig. 2 shows the rotor angle of the synchronous generators relative to the system average angle, with removed mean. We observe that 456 of 544 synchronous generators present coherent dynamics, whereas 88 of 544 synchronous generators do not contribute at all to the dynamics; see constant line at zero degrees in Fig. 2.

Upon application of the KMD explained in Section III, the 10 most important Koopman eigenvalues–i.e., the ones with the smaller damping coefficient–are shown in Fig. 3. They were estimated using 10 seconds of rotor speed estimates. The black crosses indicate results obtained with all 544 estimates

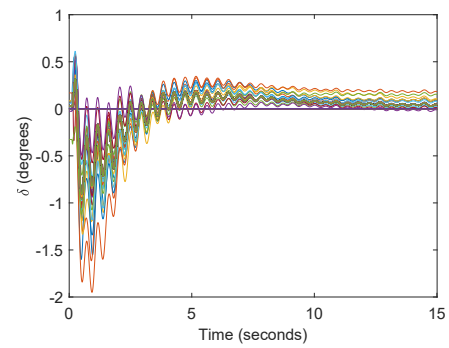

Fig. 2. Rotor angle, δ, of the 544 synchronous generators relative to system average angle, after removing the mean.

obtained from the decentralized DSE (assuming we have local PMU measurements), whereas the blue circles indicate results obtained with 240 principled selected estimates from the sparse state measurement selection technique explained in Section IV. The remaining 5 seconds of the time domain simulation are used for testing. We consider three different scenarios, as presented next.

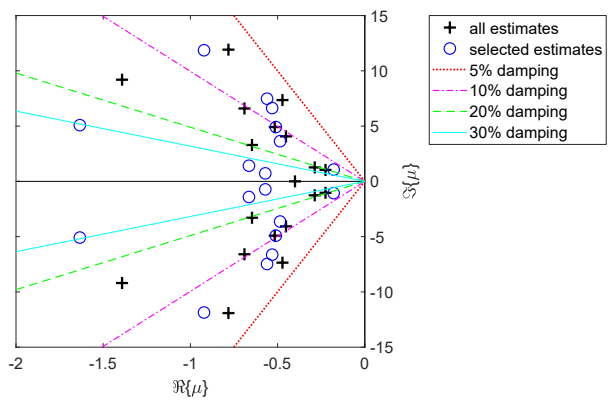

Fig. 3. The Koopman modes calculated using estimates of the rotor speed of the synchronous generators.

1) No outliers: The results are shown in Fig. 4a. *True state*, *received state estimate*, and *filtered state estimate*, respectively, refer to the outcome of the time-domain simulation, the data received from the robust model-based decentralized DSEs, and the outcome of the robust KKF.

2) Impulsive noise: The results are shown in Fig. 4b. We observe that the robust KKF is able to suppress the impulsive noise.

3) Loss of the communication link with a decentralized DSE: The results are shown in Fig. 4c. This case demonstrates the forecasting capability of the robust KKF.

VI. Conclusions and Future Research

The proposed hybrid framework offers a balance between model-based and data-driven methods, and it has several important advantages compared to other methodologies. It is completely independent of the network model, does not attempt to model the dynamics of the loads, and, most importantly, does not depend on the infrastructure that is exclusively available at the control centers.

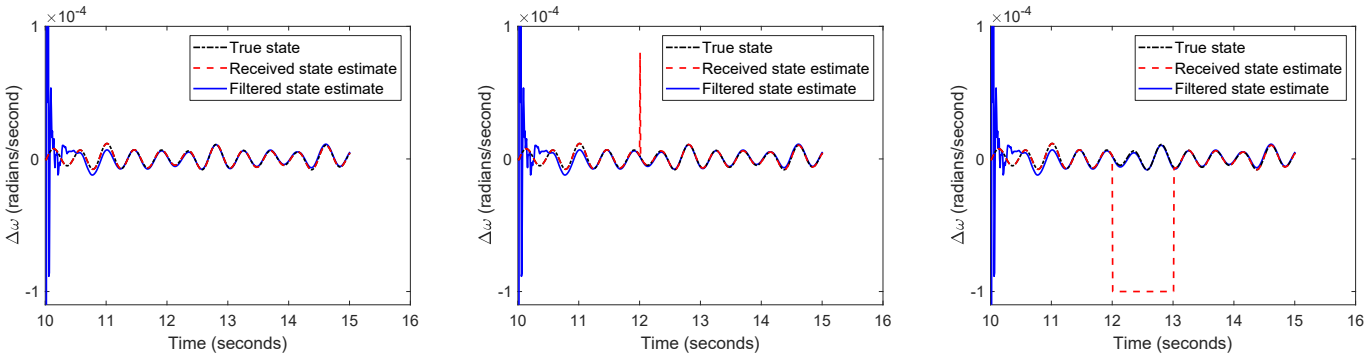

(a) (b) (c)

Fig. 4. Rotor speed deviation, $\Delta\omega$, of the synchronous generator 4. (a) No outlier. (b) Impulsive noise at $t = 12$ seconds. (c) Loss of communication with the decentralized DSE between $t = 12$ and $t = 13$ seconds.

Although promising, the proposed approach requires further investigations. One important aspect is the system observability at the upper level, i.e., the sparse selection must be conditioned to a certain degree of redundancy. We will rely on the correspondence between the Koopman operator and the Lie derivatives to pursue this effort. In addition, the estimation of the KEFs [36] is an important open problem and must be addressed. Future work will also look into the applicability of using other observables from sensors in the upper level system identification by either partially or completely bypassing the lower level DSE in certain scenarios to gain increased agility.

References

[1] S. Neumann et al., "Everything's Talking to Each Other: Smart Meters Generate Big Data for Utilities and Customers," *IEEE Power Energy Mag.*, vol. 14, no. 1, pp. 40–47, Jan 2016.

[2] A. von Meier et al. "Precision Micro-Synchrophasors for Distribution Systems: A Summary of Applications," *IEEE Trans. Smart Grid*, vol. 8, no. 6, pp. 2926–2936, Nov 2017.

[3] M. Henderson, "We Have the Data: Making It Work for Us [From the Editor]," *IEEE Power Energy Mag.*, vol. 16, no. 3, pp. 4–100, May 2018.

[4] J. P. Chaves-Avila et al., "The Green Impact: How Renewable Sources Are Changing EU Electricity Prices," *IEEE Power Energy Mag.*, vol. 13, no. 4, pp. 29–40, July 2015.

[5] B. Kroposki et al., "Achieving a 100% Renewable Grid: Operating Electric Power Systems with Extremely High Levels of Variable Renewable Energy," *IEEE Power Energy Mag.*, vol. 15, no. 2, pp. 61–73, March 2017.

[6] G. Gross and F. D. Galiana, "Short-term load forecasting," *Proc. of the IEEE*, vol. 75, no. 12, pp. 1558–1573, Dec 1987.

[7] D. W. Bunn, "Forecasting loads and prices in competitive power markets," *Proc. of the IEEE*, vol. 88, no. 2, pp. 163–169, Feb 2000.

[8] G. K. Venayagamoorthy, K. Rohrig, and I. Erlich, "One Step Ahead: Short-Term Wind Power Forecasting and Intelligent Predictive Control Based on Data Analytics," *IEEE Power Energy Mag.*, vol. 10, no. 5, pp. 70–78, Sept 2012.

[9] A. Tuohy et al., "Solar Forecasting: Methods, Challenges, and Performance," *IEEE Power Energy Mag.*, vol. 13, no. 6, pp. 50–59, Nov 2015.

[10] M. Netto and L. Mili, "Robust Koopman Operator-based Kalman Filter for Power Systems Dynamic State Estimation," in *IEEE Power Energy Soc. Gen. Meeting*, August 2018, pp. 1–5.

[11] M. Netto and L. Mili, "A Robust Data-Driven Koopman Kalman Filter for Power Systems Dynamic State Estimation," *IEEE Trans. Power Syst.*, vol. 33, no. 6, pp. 7228–7237, Nov 2018.

[12] J. Zhao et al., "Power System Dynamic State Estimation: Motivations, Definitions, Methodologies and Future," *IEEE Trans. Power Syst.*, 2018.

[13] C. W. Rowley et al., "Spectral analysis of nonlinear flows," *Journal of Fluid Mechanics*, vol. 641, pp. 115–127, 2009.

[14] M. Netto, Y. Susuki, and L. Mili, "Data-Driven Participation Factors for Nonlinear Systems Based on Koopman Mode Decomposition," *IEEE Control Systems Letters*, vol. 3, no. 1, pp. 198–203, January 2019.

[15] E. J. Candès and M. B. Wakin, "An Introduction To Compressive Sampling," *IEEE Signal Proc. Mag.*, vol. 25, no. 2, pp. 21–30, March 2008.

[16] S. L. Brunton et al., "Compressed sensing and dynamic mode decomposition," *Journal of Computational Dynamics*, vol. 2, no. 2, pp. 165–191, 2015.

[17] K. Manohar et al., "Data-Driven Sparse Sensor Placement for Reconstruction: Demonstrating the Benefits of Exploiting Known Patterns," *IEEE Control Systems*, vol. 38, no. 3, pp. 63–86, June 2018.

[18] M. Ilić and S. Liu, *Hierarchical Power Systems Control: Its Value in a Changing Industry*. Springer, 1996.

[19] H. Modir and R. A. Schlueter, "A Dynamic State Estimator for Dynamic Security Assessment," *IEEE Trans. Power App. Syst.*, vol. PAS-100, no. 11, pp. 4644–4652, Nov 1981.

[20] E. Ghahremani and I. Kamwa, "Dynamic State Estimation in Power System by Applying the Extended Kalman Filter With Unknown Inputs to Phasor Measurements," *IEEE Trans. Power Syst.*, vol. 26, no. 4, pp. 2556–2566, Nov 2011.

[21] E. Ghahremani and I. Kamwa, "Online State Estimation of a Synchronous Generator Using Unscented Kalman Filter From Phasor Measurements Units," *IEEE Trans. Energy Conversion*, vol. 26, no. 4, pp. 1099–1108, Dec 2011.

[22] M. Netto, J. Zhao, and L. Mili, "A robust extended Kalman filter for power system dynamic state estimation using PMU measurements," in *IEEE Power Energy Soc. Gen. Meeting*, July 2016, pp. 1–5.

[23] J. Zhao, M. Netto, and L. Mili, "A Robust Iterated Extended Kalman Filter for Power System Dynamic State Estimation," *IEEE Trans. Power Syst.*, vol. 32, no. 4, pp. 3205–3216, July 2017.

[24] F. Dörfler and F. Bullo, "Kron Reduction of Graphs With Applications to Electrical Networks," *IEEE Trans. Circuits and Systems I: Regular Papers*, vol. 60, no. 1, pp. 150–163, Jan 2013.

[25] J. H. Chow, *Power System Coherency and Model Reduction*. Springer, 2013.

[26] "Load representation for dynamic performance analysis," *IEEE Trans. Power Syst.*, vol. 8, no. 2, pp. 472–482, May 1993.

[27] M. Netto and L. Mili, "A Robust Prony Method for Power System Electromechanical Modes Identification," in *IEEE Power Energy Soc. Gen. Meeting*, July 2017, pp. 1–5.

[28] M. Netto and L. Mili, "Robust Data Filtering for Estimating Electromechanical Modes of Oscillation via the Multichannel Prony Method," *IEEE Trans. Power Systems*, vol. 33, no. 4, pp. 4134–4143, July 2018.

[29] A. K. Singh and B. C. Pal, "Decentralized Dynamic State Estimation in Power Systems Using Unscented Transformation," *IEEE Trans. Power Syst.*, vol. 29, no. 2, pp. 794–804, March 2014.

[30] E. Ghahremani and I. Kamwa, "Local and Wide-Area PMU-Based Decentralized Dynamic State Estimation in Multi-Machine Power Systems," *IEEE Trans. Power Systems*, vol. 31, no. 1, pp. 547–562, Jan 2016.

[31] Z. Huang et al., "Application of extended Kalman filter techniques for dynamic model parameter calibration," in *IEEE Power Energy Soc. Gen. Meeting*, July 2009, pp. 1–8.

[32] A. Paul, I. Kamwa, and G. Joos, "Centralized Dynamic State Estimation Using a Federation of Extended Kalman Filters with Intermittent PMU Data from Generator Terminals," *IEEE Trans. Power Syst.*, 2018.

[33] A. Surana and A. Banaszuk, "Linear observer synthesis for nonlinear systems using Koopman Operator framework," *IFAC-PapersOnLine*, vol. 49, no. 18, pp. 716–723, 2016.

[34] M. A. Gandhi and L. Mili, "Robust Kalman Filter Based on a Generalized Maximum-Likelihood-Type Estimator," *IEEE Trans. Signal Proc.*, vol. 58, no. 5, pp. 2509–2520, May 2010.

[35] A. B. Birchfield et al., "Grid Structural Characteristics as Validation Criteria for Synthetic Networks," *IEEE Trans. Power Syst.*, vol. 32, no. 4, pp. 3258–3265, July 2017.

[36] M. Korda and I. Mezić, "Learning Koopman eigenfunctions for prediction and control: the transient case," *arXiv preprint*, arXiv:1810.08733v1, 2018.